IEEE Photonics Journal
An IEEE Photonics Society Publication

Open Access

Influence of Collimation on Alignment Accuracy in Proximity Lithography

Volume 6, Number 4, August 2014

Nan Wang
Wei Jiang
Jiangping Zhu
Yan Tang
Wei Yan
Junmin Tong
Song Hu

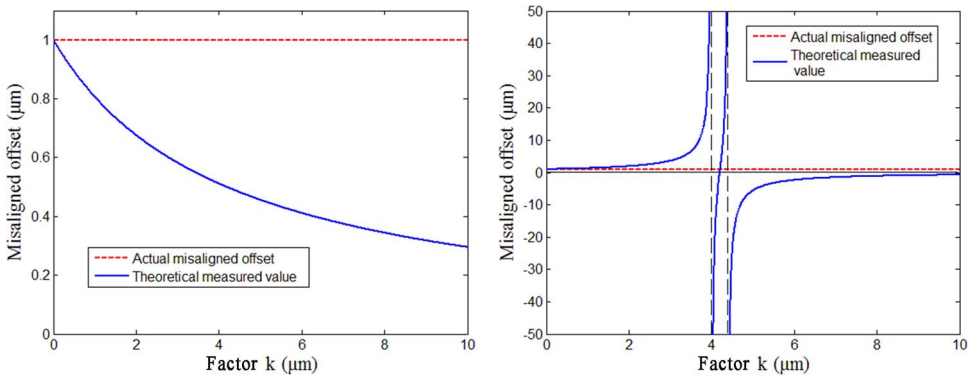

The influence of divergent light

The influence of convergent light

DOI: 10.1109/JPHOT.2014.2345878
1943-0655

Influence of Collimation on Alignment Accuracy in Proximity Lithography

Nan Wang,[1,2] Wei Jiang,[1] Jiangping Zhu,[3] Yan Tang,[1] Wei Yan,[1] Junmin Tong,[4] and Song Hu[1]

[1]State Key Laboratory of Optical Technologies for Microfabrication, The Institute of Optics and Electronics, Chinese Academy of Sciences, Chengdu 610209, China
[2]University of Chinese Academy of Sciences, Beijing 100039, China
[3]School of Optoelectronic Information, University of Electronic Science and Technology of China, Chengdu 610054, China
[4]Xuchang Vocational and Technical College, Xuchang 461000, China

DOI: 10.1109/JPHOT.2014.2345878

Manuscript received July 17, 2014; accepted July 31, 2014. Date of publication August 7, 2014; date of current version August 20, 2014. This work was supported by the National Natural Science Foundation of China under Grant 61274108 and Grant 61274114. Corresponding author: N. Wang (e-mail: 705679317@qq.com).

Abstract: The alignment method based on moiré imaging has been wildly used for its high accuracy of physical measurement, which utilized the phase of moiré fringe to measure the relative linear displacement between the mask and the wafer. However, this method is only theoretically accurate due to the affection of certain parameters, such as the optical beam collimation. In this paper, the influence of collimation on the alignment accuracy is thoroughly analyzed. The theoretical analyses and simulation results indicate that the alignment accuracy, which was observed just behind the test grating, is sensitive to the divergence or convergence angle of incident light. On this basis, the method for the error correction is proposed and confirmed.

Index Terms: Collimation, moiré fringe, lithography alignment.

1. Introduction

The proximity photolithography, nanoimprint lithography, and x-ray lithography have proven to be valuable tools to the fabrication of wide varieties of optoelectronic and electronic devices, such as the master or mold fabrication in soft lithography [1], optical fabrication for micro optical components [2], [3] and photonic crystal [4], [5], etc. Hereinto, one of the most essential steps is the optical alignment of wafer and mask. By now, several alignment techniques have been employed to detect the displacement deviation or aligned position [6]–[11]. Recently, a moiré imaging method that encodes the aligned point into the spatial phase of moiré fringes has been wildly used due to the high sensitivity and accuracy [9]–[11]. It is well known that the detected results by this method are affected by certain factors other than necessary information, such as the tilt angle of the moiré fringes [12], the measurement accuracy of Talbot imaging positions [13]–[15], and the angle between two unparallel diffraction grating planes [16], [17]. Besides, other parameters including the optical beam collimation, which also plays an important role in the measurement results, has been rarely reported.

Generally speaking, all the alignment process based on moiré metrology has been discussed under the ideal condition of incident light with perfect collimation. However, it is still very difficult

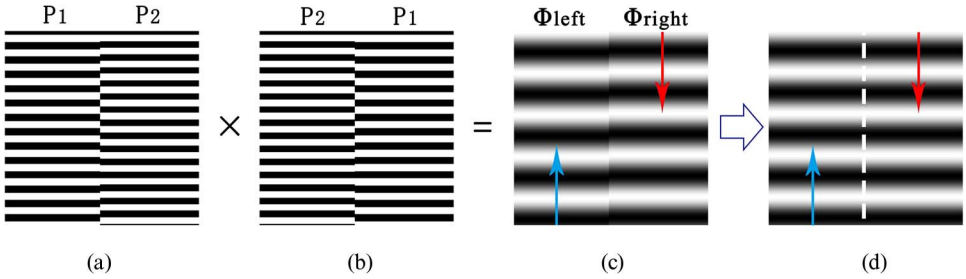

Fig. 1. Alignment marks using mosaic gratings. (a) Mask alignment mark. (b) Wafer alignment mark. (c) Misaligned moiré fringe. (d) Aligned moiré fringe. In (c) and (d), the red and blue arrows represent the shifting direction of moiré fringe on the left and right, and the φ_{Left} and φ_{Right} are the phase distribution of moiré fringe on the left and right.

to obtain a perfect collimated beam in a practical measurement, the influence of the collimation parameter of incident light on the alignment accuracy must be considered under various strict conditions. Herein, this paper mainly studies how the collimation affects its phase distribution and then the alignment accuracy. On this basis, the method for error correction is proposed and confirmed.

2. Theoretical Analysis

In the moiré alignment method based on dual gratings, the mask alignment mark and the wafer alignment mark are comprised of two mosaic linear gratings with close periods T_1 and T_2 $(T_1 > T_2)$, as shown in Fig. 1(a) and (b). The most resolvable (1, −1) moiré fringe with the lowest spatial frequency or the maximum period, occur at the surface of two superposed gratings at the incidence of a plant wave, due to the interference of diffraction waves from two gratings, shown in Fig. 1(c) and (d). The complex amplitude of transmittance generated can be given as

$$E_{(1,-1)}(x,y) = \sum_{n=-\infty}^{+\infty} A_n B_n \exp[i2\pi n(f_1 - f_2)y] \tag{1}$$

where A_nB_n, $f_1 = 1/T_1$ and $f_2 = 1/T_2$ represent the Fourier coefficient, fundamental frequencies of two gratings, respectively.

For the aligned moiré fringe, as shown in Fig. 1(d), the corresponding phase distribution on the left and right can be written as

$$\varphi_{\text{Left}} = \varphi_{\text{right}} = 2\pi(f_1 - f_2)y. \tag{2}$$

Assuming that the actual misaligned offset between the mask and the wafer is written by Δy, the change of phases φ_{Left} and φ_{Right} in Fig. 1(c) will be expressed as

$$\Delta\varphi_{\text{Left}} = 2\pi[f_1(y+\Delta y) - f_2 y] - 2\pi(f_1 - f_2)y = \frac{2\pi\Delta y}{T_1}$$
$$\text{and} \quad \Delta\varphi_{\text{Right}} = 2\pi[f_1 y - f_2(y+\Delta y)] - 2\pi(f_1 - f_2)y = \frac{-2\pi\Delta y}{T_2}. \tag{3}$$

In addition, the phase difference between two moiré fringes can be denoted as

$$\Delta\varphi_{Moire} = \Delta\varphi_{\text{Left}} - \Delta\varphi_{\text{Right}} = 2\pi\Delta y\left(\frac{1}{T_1} + \frac{1}{T_2}\right). \tag{4}$$

From (4), the actual misaligned offset Δy can be expressed as

$$\Delta y = \frac{\Delta\varphi_{Moire}}{2\pi\left(\frac{1}{T_1} + \frac{1}{T_2}\right)}. \tag{5}$$

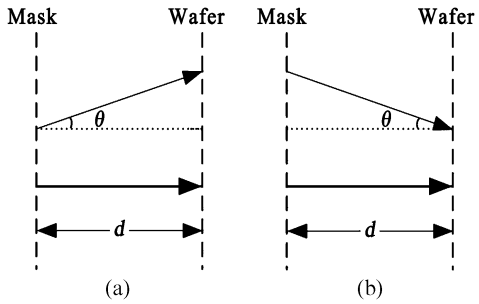

Fig. 2. The schematic of alignment with (a) divergent light and (b) convergence angle.

When the plane wave becomes spherical, the self-image of mask alignment mark becomes magnified or demagnified, depending on whether the incident light is divergent or convergent, shown in Fig. 2. In the case described here, (3) and (4) should be modified as

$$\Delta\varphi_{Left} = \frac{2\pi\Delta y}{T_1 + \theta d} \quad \text{and} \quad \Delta\varphi_{Right} = \frac{-2\pi\Delta y}{T_2 + \theta d} \tag{6}$$

$$\Delta\varphi_{Moire} = \Delta\varphi_{Left} - \Delta\varphi_{Right} = \frac{2\pi\Delta y(T_1 + T_1 + 2\theta d)}{(T_1 + \theta d)(T_2 + \theta d)} \tag{7}$$

where θ represents the divergence or convergence angle, and d is the distance of the gap between the wafer alignment mark and the mask alignment mark. Additionally, the θ is a positive value for the divergent light or a negative value for the convergent light.

The relationship between the theoretical measured value ΔY and the actual misaligned offset Δy is

$$\Delta Y = \frac{\Delta\varphi_{Moire}}{2\pi(f_1 + f_2)} = \frac{T_1 T_2(T_1 + T_2 + 2\theta d)}{(T_1 + T_2)(T_1 + \theta d)(T_2 + \theta d)}\Delta y = \frac{T_1 T_2(T_1 + T_2 + 2k)}{(T_1 + T_2)(T_1 + k)(T_2 + k)}\Delta y \tag{8}$$

where the factor k is the product of θ and d.

According to (8), some discussions are given as follows.

1) The deform degree of moiré fringes depends on the factor k, which is the product of the divergence or convergence angle and the gap distance. Therefore, in the case of noncollimated incident light, the alignment method based on dual gratings no longer has the advantage that the accuracy is insensitive to the gap distance.
2) For the collimated light, $k = 0$, then Eq. (8) is written as $\Delta Y = \Delta y$. Under such ideal condition assumed by most of moiré alignment methods, the error between the theoretical measured value and the actual misaligned offset is zero, which is applicable for the high accurate alignment in lithography.
3) For the divergent light, $\theta > 0$, then $k > 0$. The theoretical measured value monotonically decreases from the actual misaligned offset *to* zero with the increased factor k, as shown in Fig. 3(a). In such case, the theoretical measured value is smaller than the actual misaligned offset, making the moiré alignment methods unfavorable for the calculation of accurate alignment.
4) For the convergent light, $\theta < 0$, then $k < 0$. One can see that the curve becomes complex in Fig. 3(b). Firstly, the theoretical measured value becomes infinite at two extreme points, in which of the situation one grating of the mask alignment mark focuses into a line and the moiré fringe disappears. Secondly, there exists a segmentation point: to the right of it, the theoretical measured value and actual misaligned offset are opposite in sign, resulting in a totally misjudgment of misalignment state. Thirdly, comparing with the divergent light, the error between the theoretical measured value and actual misaligned offset under this

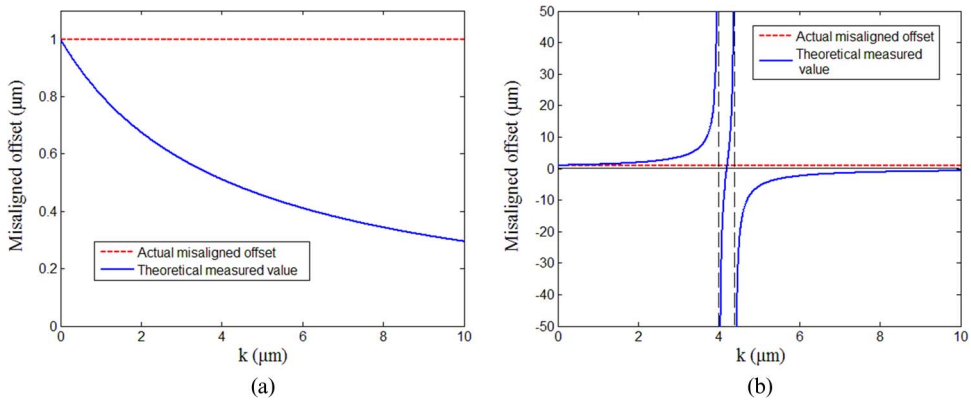

Fig. 3. ($(\Delta y = 1\ \mu\text{m})$ ($T_1 = 4\ \mu\text{m}$, $T_2 = 4.4\ \mu\text{m}$)) Variations of the theoretical measured value with the factor k for (a) the divergent light and (b) the convergent light.

condition is more sensitive to the factor k, which is more unsuitable for the alignment with high accuracy.

5) It is well known that the ideal collimated light is impossible to achieve. Accordingly, the method for the error correction is proposed by this paper. Based on Eq. (8), we can conveniently modify the theoretical measured value into actual misaligned offset by measuring the divergence or convergence angle and gap distance. In this way, the accuracy of modification lies on the measurement accuracy of divergence or convergence angle and gap distance.
6) For the high-precision measurement of divergence or convergence angle, some special test instruments could be adopted. However, because of the influence of noncollimated light on the period of moiré fringes, the information about the divergence or convergence angle could be gathered from the fringes themselves by the use of the Fourier-transform algorithm (FTA) [18].
7) The error caused by the collimation is more complex and serious than other error sources. For example, the error caused by the tilt angle only gives rise to the diminution of period of moiré fringes [16], [17] while the error caused by the collimation leads to the diminution and amplification of period of moiré fringes; the error caused by small relative rotations between gratings is periodic and limited [12], but the error caused by the collimation is boundless and sign reversing.

3. Numerical Simulation

To confirm the validity of theoretical discusses, numerical simulations are performed to achieve the alignment state on the platform of MATLAB 7.1. In the simulation, we adopt two composite gratings with periods of $T_1 = 4\ \mu\text{m}$, $T_2 = 4.4\ \mu\text{m}$, separated by an adjustable gap. After the acquisition of moiré fringes by drawing with computer, the FTA is used to determine the phase distribution in the vertical direction [19]–[21].

3.1. Alignment Case 1: The Collimated Light

For the verification of the second discussion in Section 2, ten groups of simulations are carried out with collimated light. In each group, the numerical simulation is performed to measure the misaligned offset individually under the same condition that the actual misaligned offset and gap distance are respectively 0.1 μm and 100 μm.

The moiré fringe patterns caused by the collimated light are demonstrated in Fig. 4(a) while the simulation results are shown in Fig. 4(b). By comparing the simulation results with the actual misaligned offset, the maximum absolute error and the maximum relative error are

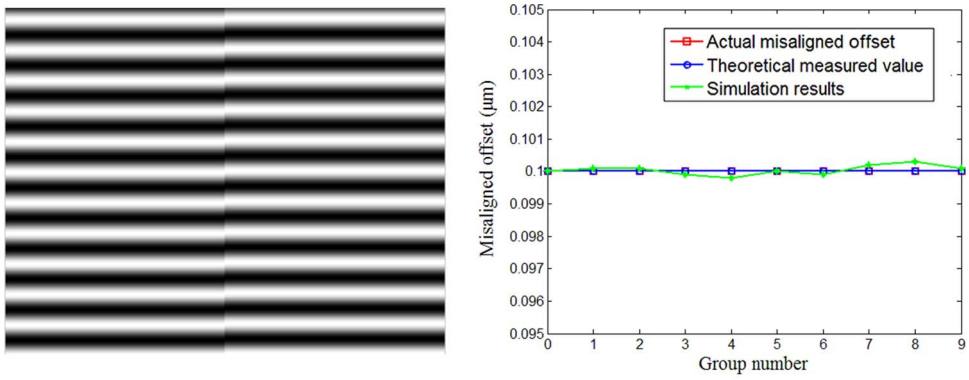

Fig. 4. Alignment case 1 (collimated light). (a) Moiré fringe patterns and (b) the simulation results.

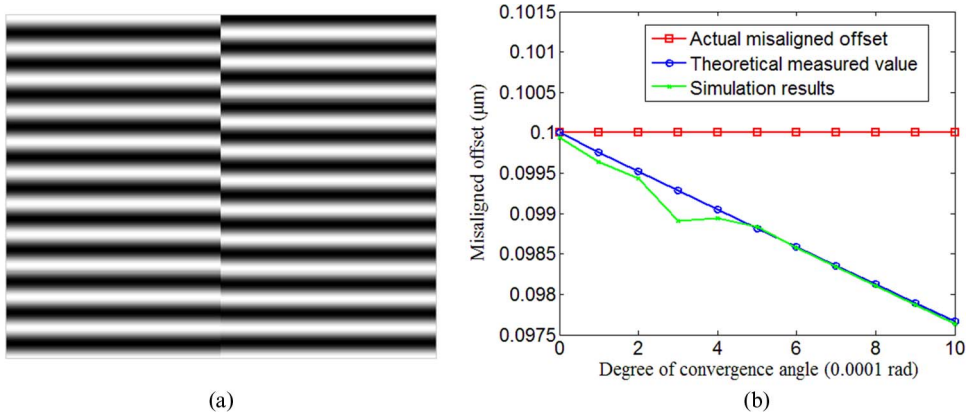

Fig. 5. Alignment case 2 (divergent light). (a) Moiré fringe patterns (b) variations of the simulation results with divergence angle.

respectively 0.0003 μm and 0.3%, which are mainly caused by the limitation of phase extraction algorithm.

3.2. Alignment Case 2: The Divergent Light

To examine the correctness of the third discussion in Section 2, the simulation is performed with several increased divergent angles in the case of divergent light. In the simulation, the gap distance of 100 μm is a fixed value while the actual misaligned offset of 0.1 μm is the value need to be measured. Considering that the experimental illuminating beam is collimated beforehand, we will discuss only the alignment case by means of moiré fringe that are generated by divergent light with a small angle.

The moiré fringe pattern caused by the divergent light with an angle of 0.0001 rad is demonstrated in Fig. 5(a) and the simulation results are given in Fig. 5(b). It is obvious that the simulation results are in agreement with the theoretical measured values, which gradually decreased from the actual misaligned offset with the increase of convergence angle. For the small angular displacements $\theta \in [0, 0.0006 \text{ rad}]$ shown in Fig. 5(b), the error is also very large, which is not favorable for the calculation of accuracy alignment.

For example, when $\theta = 0.0006$ rad, the absolute error is 0.0015 μm, and the relative error reaches 1.5%. While in the ideal state of collimated light, the absolute error is 0.0001 μm, and the relative error is only 0.1%.

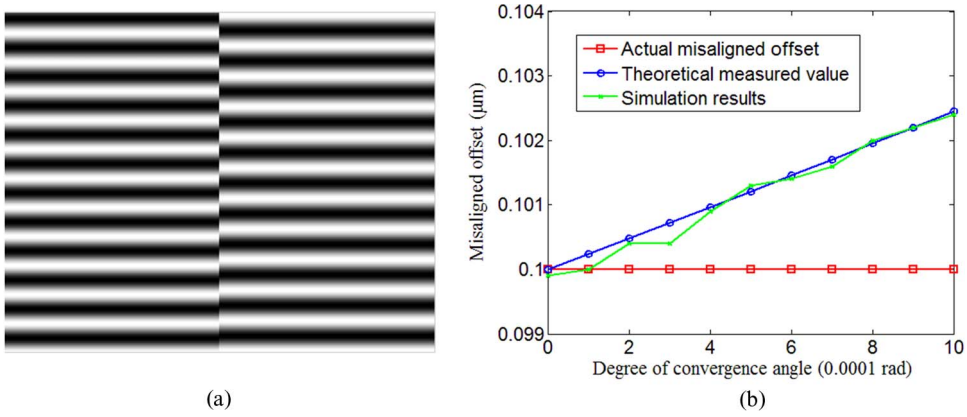

Fig. 6. Alignment case 2 (convergent light): (a) moiré fringe patterns and (b) variations of the simulation results with convergence angle.

3.3 Alignment Case 3: The Convergent Light

Although the relationship between the theoretical measured value and actual misaligned offset is very complex in the case of convergent light, the theoretical measured value becomes monotonous and limited in terms of the small convergent angles. For the demonstration of this conclusion, a simulation is performed to measure the misaligned offset for several values of convergent angle varying between 0 and 0.001 rad. Additionally, the gap distance and actual misaligned offset are fixed to be 100 μm and 0.1 μm, respectively.

Fig. 6(a) is the moiré fringe patterns of the convergent light with a convergence angle of 0.0001 rad. It can be found that the period of moiré fringes changes with the convergence angle, which will greatly affect the phase distribution of moiré fringes and the identification of aligned position or state.

It is apparently that the good agreement between the theoretical measured values and simulation results obtained in Fig. 6(b). The curve indicates that the simulation results gradually deflect from the actual misaligned offset with the increased convergence angle, bringing about a large error. Supposed that $\theta = 0.0001$ rad, both the simulation result and theoretical measured value have the same relative error of 2.4% with regard to the actual misaligned offset.

3.4. Other Influences

The first discussion in Section 2 is proven by the next two groups of numerical simulations. In the first group, the angle of divergent light and actual misaligned offset are set as 0.0001 rad and 0.1 μm, respectively. The evenly spaced increase is then performed by the gap distance while the corresponding moiré fringe is recorded to achieve the misaligned offset. In the other group, the divergent light is replaced by the convergent light and the same operation is performed as the first group.

The simulation results of the first group are demonstrated in Fig. 7(a) while the simulation results of the second group are given in Fig. 7(b). The curves of two groups are in good agreement with the theoretical measured values. Typically, when the gap distance is 500 μm, the maximum relative errors of two groups are 1.23% and 1.19%, respectively.

4. Experiment

Based on the discussion about the method for error correction in Section 2, an alignment experiment is performed to measure the misaligned offset, as shown in Fig. 8. At first, one set of alignment marks with periods of T_1 (4 μm) and T_2 (4.4 μm) is designed. A laser beam with wavelength of 632.8 nm is expanded by use of a 40$\times$ microscope objective and a pinhole of 5 μm diameter, and then incident upon a collimation lens mounted upon a precision translation stage

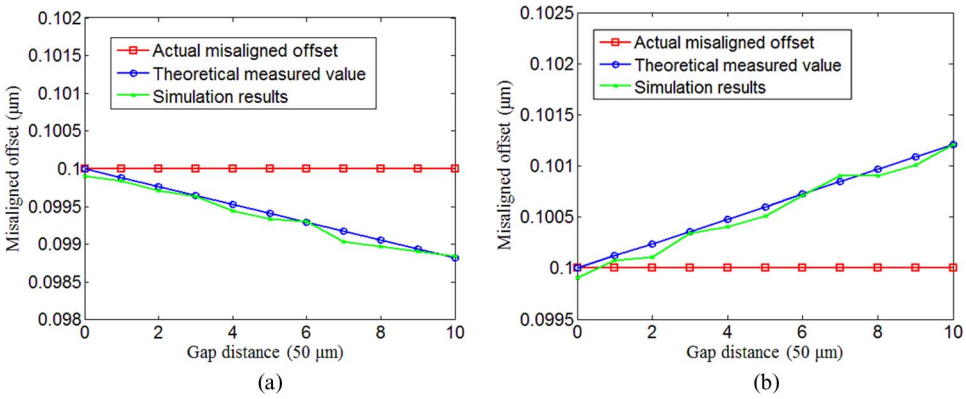

Fig. 7. Variations of the simulation results with the gap distance. (a) The divergent light and (b) the convergent light.

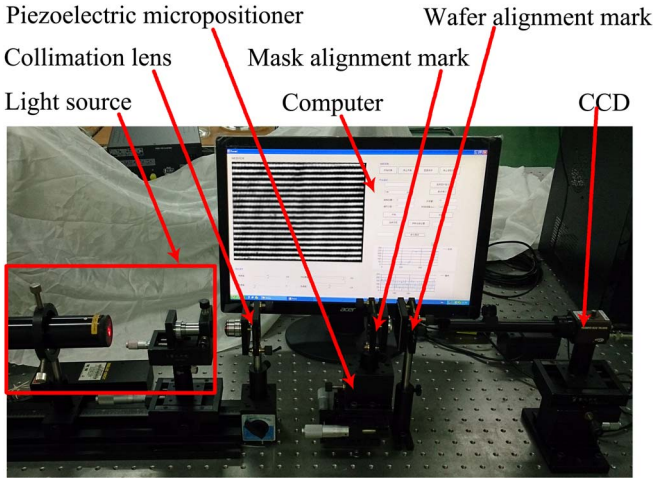

Fig. 8. The experimental setup.

with a least count of 1 μm. By adjusting the lens position, the incident beam with one of the three collimation states illuminates a mask which was placed in front of a wafer, and the moiré fringe patterns are recorded by a CCD camera (WAT902H). The misaligned offset between the mask and the wafer is adjusted by a piezoelectric micro positioner with a resolution of 2 nm.

In the experiment, the gap distance is adjusted to about 100 μm. When the mask and the wafer are adjusted to be parallel, two sets of linear moiré fringes are obtained. After that, we adjust the incident light into collimated light by the movement of the collimation lens. This process continues until the period of two sets of moiré fringes are equal, which means the collimated light is achieved. Next, the misaligned offset between the mask and the wafer is first remedied to zero and then 0.1 μm by the use of the piezoelectric micro positioner. At this moment, the position of collimating lens and corresponding moiré fringe patterns are recorded for the first time. Then the collimation lens moves in the same or opposite direction until the noncollimated light is generated, and the position of collimation lens and corresponding moiré fringe patterns are again recorded. The distance between the two positions is the defocusing distance, through which the divergence or convergence angle could be obtained.

Three groups of experiments are performed, which correspond to the collimated light, divergent light and convergent light, respectively. To improve the accuracy in phase extraction, the captured patterns are cut with integral number of moiré fringe period, as shown in Figs. 9(a)–11(a). For the

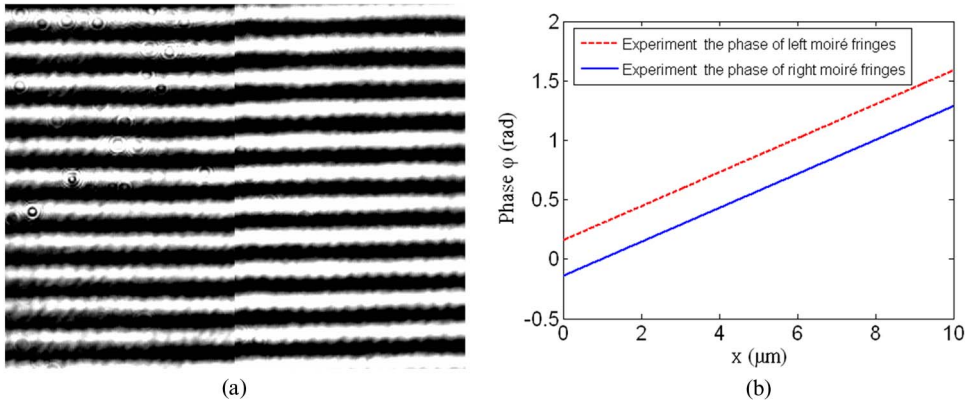

Fig. 9. The moiré fringe patterns in experiment. (a) Moiré fringe patterns of collimated light. (b) $\varphi(x)$ against x by using FTA.

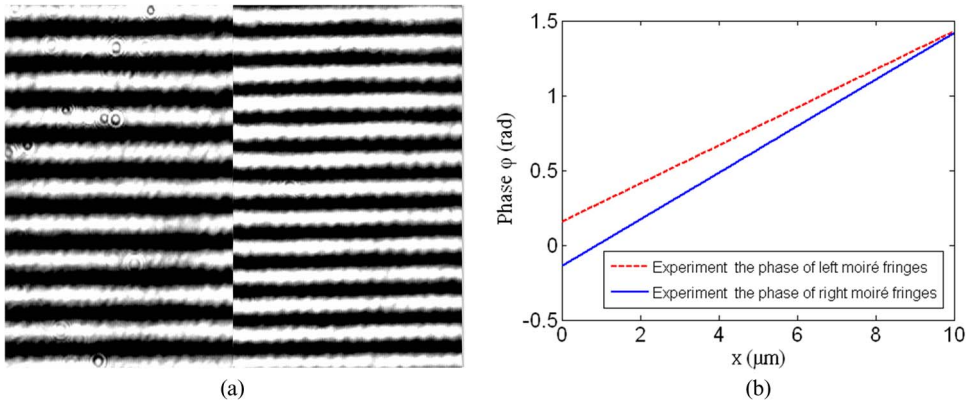

Fig. 10. The moiré fringe patterns in experiment. (a) Moiré fringe patterns of divergent light. (b) $\varphi(x)$ against x by using FTA.

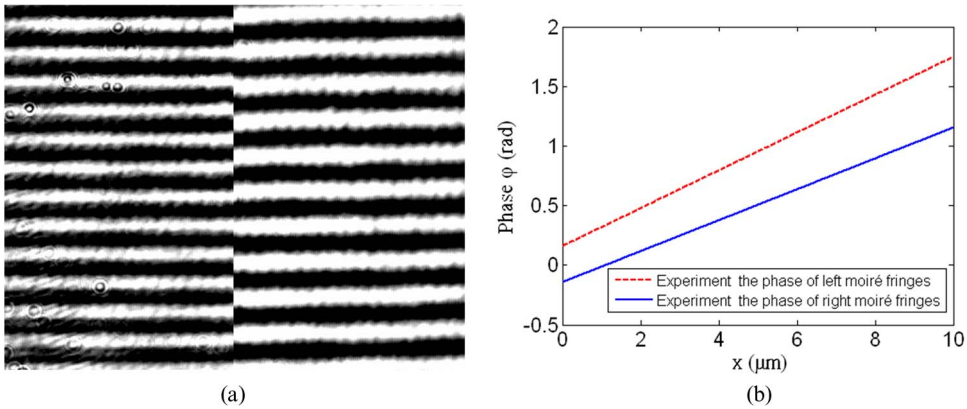

Fig. 11. The moiré fringe patterns in experiment. (a) Moiré fringe patterns of convergent light. (b) $\varphi(x)$ against x by using FTA.

acquisition of the information about misaligned offset, the FTA is used to analysis the moiré fringes. The corresponding phase distributions are shown in Figs. 9(b)–11(b) while experimental results are listed in Table 1. Because of the large errors cased by divergent light or convergent

TABLE 1

Experimental results and modification values

Collimation state	Degree of angle (rad)	Actual value	Experimental results			Modification values		
		Misaligned offset(μm)	Misaligned offsets(μm)	Absolute error(μm)	Percentage errors(%)	Misaligned offset(μm)	Absolute errors(μm)	Percentage errors(%)
Collimated light	0	0.1	0.1001	0.0001	0.1	0.1001	0.0001	0.1
Divergent light	0.0004	0.1	0.0988	0.0012	1.2	0.0997	0.0003	0.3
Convergent light	0.0004	0.1	0.1012	0.0012	1.2	0.1002	0.0002	0.2

light, the experimental results are modified by the method for error correction and the modified values are also listed in Table 1. By comparing with the experimental results and modified values, it can be seen that the improved method proposed in this paper is valid.

5. Conclusion

The Influence of collimation on the alignment accuracy was deeply analyzed and verified by the simulation and experiment. The simulation results indicate that the phase distribution of moiré fringe is very sensitive to the divergence or convergence angle of the incident light, resulting in the poor accuracy of alignment and displacement detecting and sensing. The alignment method with collimated light, by contrast, not only has a high accuracy, but also is easy to identify the alignment state, which shows an acceptable agreement with the actual value. Moreover, the experimental results have verified that the method for error correction can be performed with a good degree of accuracy, making it well suited for the application in a real system. Last but not the least, it should be noted that these findings can be also applied to other correlated fields, not necessarily limited to the lithography.

References

[1] G. M. Whitesides, E. Ostuni, S. Takayama, X. Jiang, and D. E. Ingber, "Soft lithography in biology and biochemistry," *Annu. Rev. Biomed. Eng.*, vol. 3, no. 1, pp. 335–373, Aug. 2001.
[2] C. Xie *et al.*, "Toward two-dimensional nanometer resolution hard X-ray differential-interference-contrast imaging using modified photon sieves," *Opt. Lett.*, vol. 37, no. 4, pp. 749–751, Feb. 2012.
[3] Y. Zhang, N. Gao, and C. Xie, "Using circular Dammann gratings to produce impulse optic vortex rings," *Appl. Phys. Lett.*, vol. 100, no. 4, pp. 041107-1–041107-4, Jan. 2012.
[4] P. Yao, G. Schneider, D. Prather, E. Wetzel, and D. O'Brien, "Fabrication of three-dimensional photonic crystals with multilayer photolithography," *Opt. Exp.*, vol. 13, no. 7, pp. 2370–2376, Mar. 2005.
[5] V. Reboud *et al.*, "Lasing in nanoimprinted two-dimensional photonic crystal band-edge lasers," *Appl. Phys. Lett.*, vol. 102, no. 7, pp. 073101-1–073101-4, Feb. 2013.
[6] B. Fay, J. Trotel, and A. Frichet, "Optical alignment system for submicron X-ray lithography," *J. Vac. Sci. Technol.*, vol. 16, no. 6, pp. 1954–1958, Nov. 1979.
[7] D. C. Flanders, H. I. Smith, and S. Austin, "A new interferometric alignment technique," *Appl. Phys. Lett.*, vol. 31, no. 7, pp. 426–428, Oct. 1977.
[8] M. Suzuki and A. Une, "An optical-heterodyne alignment technique for quarter-micron X-ray lithography," *J. Vac. Sci. Technol. B, Microelectron. Nanom. Struct.*, vol. 7, no. 6, pp. 1971–1976, Nov./Dec. 1989.
[9] A. Moel, E. E. Moon, R. D. Frankel, and H. I. Smith, "Novel on-axis interferometric alignment method with sub-10 nm precision," *J. Vac. Sci. Technol. B, Microelectron. Nanom. Struct.*, vol. 11, no. 6, pp. 2191–2194, Nov./Dec. 1993.
[10] E. E. Moon and H. I. Smith, "Nanometer-precision pattern registration for scanning-probe lithographies using interferometric-spatial-phase imaging," *J. Vac. Sci. Technol. B, Microelectron. Nanom. Struct.*, vol. 24, no. 6, pp. 3083–3087, Nov./Dec. 2006.
[11] J. P. Zhu *et al.*, "Four-quadrant gratings Moiré fringe alignment measurement in proximity lithography," *Opt. Exp.*, vol. 21, no. 3, pp. 3463–3473, Feb. 2013.
[12] J. P. Zhu *et al.*, "Influence of tilt Moiré fringe on alignment accuracy in proximity lithography," *Opt. Lasers Eng.*, vol. 51, no. 4, pp. 371–381, Apr. 2013.

[13] S. Yokozeki and K. Ohnishi, "Spherical aberration measurement with a shearing interferometer using Fourier imaging and Moiré method," *Appl. Opt.*, vol. 14, no. 3, pp. 623–627, Mar. 1975.
[14] M. P. Kothiyal, K. V. Sriram, and R. S. Sirohi, "Setting sensitivity in Talbot interferometry," *Opt. Laser Technol.*, vol. 23, no. 6, pp. 361–365, Dec. 1991.
[15] C. W. Chang and D. C. Su, "An improved technique for measuring the focal length of a lens," *Opt. Commun.*, vol. 73, no. 4, pp. 257–262, Oct. 1989.
[16] Q. Liu and R. Ohba, "Effects of unparallel grating planes in Talbot interferometry," *Appl. Opt.*, vol. 38, no. 19, pp. 4111–4116, 1999.
[17] Q. Liu, R. Ohba, and S. Kakuma, "Effects of unparallel grating planes in Talbot interferometry. II," *Appl. Opt.*, vol. 39, no. 13, pp. 2084–2090, May 2000.
[18] N. Wang, Y. Tang, W. Jiang, W. Yan, and S. Hu, "Collimation sensing with differential grating and Talbot interferometry," *IEEE Photon. J.*, vol. 6, no. 3, p. 6100210, Jun. 2014.
[19] L. Huang and X. Y. Su, "Method for acquiring the characteristic parameter of the dual-spiral Moiré fringes," *Opt. Lett.*, vol. 33, no. 8, pp. 872–874, Apr. 2008.
[20] F. Xu, H. Song, and S. L. Zhou, "Fringe pattern analysis for optical alignment in nanolithography using two-dimensional Fourier transform," *Opt. Eng.*, vol. 50, no. 8, pp. 088001-1–088001-7, Aug. 2011.
[21] S. L. Zhou *et al.*, "Fourier-based analysis of Moiré fringe patterns of superposed gratings in alignment of nanolithography," *Opt. Exp.*, vol. 16, no. 11, pp. 7869–7880, May 2008.